JCTC Journal of Chemical Theory and Computation

Critical Role of the Correlation Functional in DFT Descriptions of an Agostic Niobium Complex

Dimitrios A. Pantazis,[†] John E. McGrady,*[,†] Feliu Maseras,[‡] and Michel Etienne[§]

WestCHEM, Department of Chemistry, Joseph Black Building, University of Glasgow, Glasgow G12 8QQ, U.K., Institute of Chemical Research of Catalonia (ICIQ), Avgda. Països Catalans 16, 43007, Tarragona, Spain, Unitat de Química Física, Edifici Cn, Universitat Autònoma de Barcelona, 08193 Bellaterra, Catalonia, Spain, and Laboratoire de Chimie de Coordination du CNRS, UPR 8241 liée par conventions à l'Université Paul Sabatier et à l'Institut National Polytechnique de Toulouse, 205 Route de Narbonne, Toulouse Cedex 4, France

Received February 21, 2007

Abstract: In previous studies of the agostic bonding in $Tp^{Me2}NbCl(R'CCR'')(R)$, we have made use of a hybrid QM/MM protocol (B3LYP:UFF) where the QM partition ($[Nb(Cl)(i\text{Pr})(HCCH)(NHCH_2)_3]^+$) was rather small, but the optimized structures were nevertheless in apparently good agreement with experiment. In attempting to improve this model by expanding the size of the QM region, we were surprised to discover that a full QM treatment of the whole molecule using the B3LYP functional failed to locate an agostic structure of any kind. A systematic assessment of density functionals reveals that the poor performance of B3LYP in these systems is typical of all DFT methods that do not obey the uniform electron gas (UEG) correlation limit. Those that do obey the UEG limit, in contrast, provide an excellent description of the agostic structure when the complete ligand system is treated at the QM level. The apparently good performance of our original (B3LYP:UFF) hybrid method can be traced to a cancellation of errors: the B3LYP functional underestimates the intrinsic strength of the agostic interaction relative to competing Nb−Cl π bonding, but this is offset by an additional but unphysical electrostatic component to the agostic bond introduced by the presence of a positive charge in the QM region.

Introduction

The nature of the agostic bond in transition-metal organometallic compounds continues to excite debate in the literature.[1−3] The earliest, and perhaps simplest, model of a C−H···M interaction[4] is as a 3-center 2-electron interaction between a C−H (or C−C) σ bond and an electron-deficient metal center, a picture that was supported by early studies of the β-C−H agostic interaction using Extended Hückel theory,[5] along with a more recent analysis using the Atoms in Molecules (AIM) procedure.[6] Scherer and McGrady have, however, arrived at a rather different model of the agostic bonding in electropositive d^0 metal alkyls based on hyperconjugative stabilization of the M−C bonding electrons by antibonding orbitals localized on the alkyl group.[7,8] This model is somewhat reminiscent of the early work of Eisenstein and co-workers on α-C−H agostics,[5] where delocalization of the M−C bonding electrons, in this case into vacant orbitals on the metal, was identified as the major driving force for the α-C−H agostic structure of $H_5TiCH_3^{2-}$. In more electron-rich late transition metals, back-bonding into the C−H σ* orbitals can also stabilize agostic bonds,[9] often leading to substantial elongation of the C−H bonds (∼1.25 Å[10] compared to ∼1.12 Å and ∼1.10 Å in electron-

* Corresponding author e-mail: j.mcgrady@chem.gla.ac.uk.
[†] University of Glasgow.
[‡] Institute of Chemical Research of Catalonia (ICIQ) and Universitat Autònoma de Barcelona.
[§] UPR 8241 liée par conventions à l'Université Paul Sabatier et à l'Institut National Polytechnique de Toulouse.

10.1021/ct700043w CCC: $37.00
Published on Web 05/26/2007

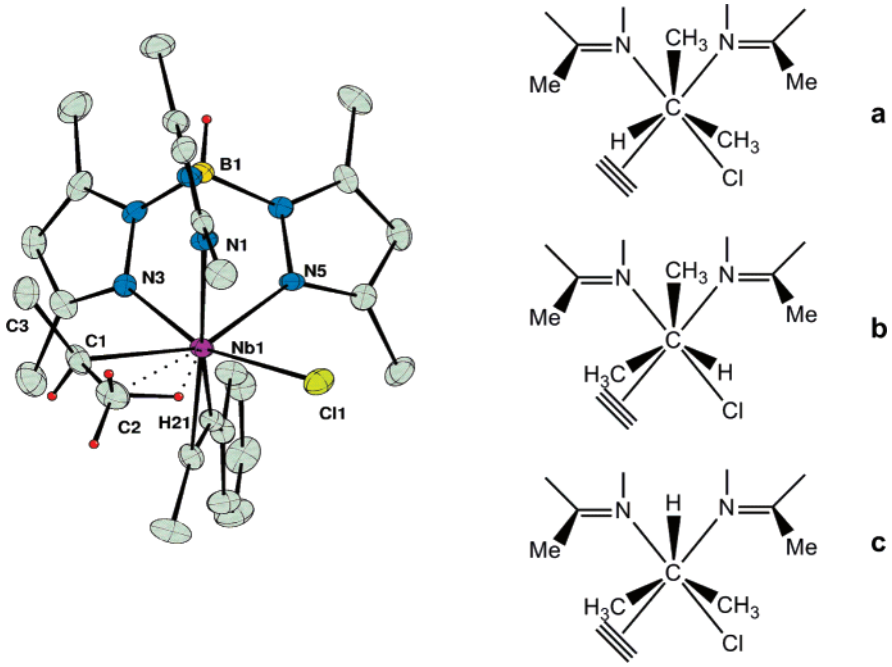

Figure 1. Crystal structure of $Tp^{Me2}NbCl(PhCCMe)iPr$ (rotamer a) and the relationship between the rotamers (a)−(c) (viewed along the Nb−C_α bond).

Scheme 1. QM/MM Partitions in Models I−III[a]

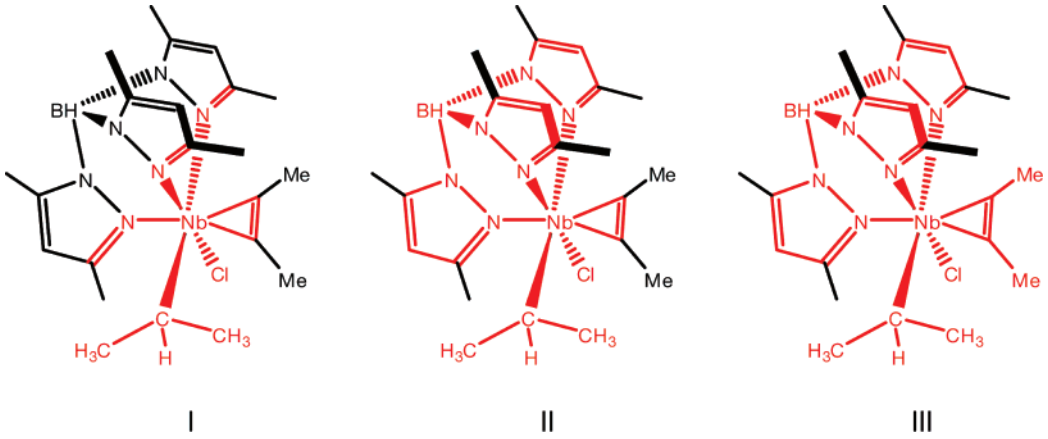

[a] The QM region is shown in red, MM in black.

deficient agostic and nonagostic C−H bonds, respectively). In light of the varied electronic mechanisms that can potentially stabilize an agostic bond, it is perhaps unsurprising that many authors have settled for a phenomenological definition based on structure rather than a specific electronic mechanism. Thus the combination of a short metal−hydrogen separation, an elongated C−H bond and relatively small angles in the M−C−C−H unit, are generally taken as indicative of an agostic structure, whatever its origin.

Over the past 8 years we have published a number of papers where we have adopted this approach to probe the agostic bonding in a series of niobium−alkyl complexes, $Tp^{Me2}NbCl(R'CCR'')(R)$ (Figure 1).[11−15] The facial $Tp^{Me2}M$ fragment provides a unique platform to investigate the nature of agostic interactions, because the pendant methyl groups define a tight steric pocket on the opposite face of the metal and so restrict rotation about the Nb−C_α bond. As a result, isomers differing only in the torsion angles about this Nb−C_α bond form distinct minima on the potential energy surface. For example, in the case of the isopropyl complex (Figure 1), rotation of the alkyl moiety generates three distinct minima (a−c), two of which (a and b) are in equilibrium in solution.

In the work described in refs 11−15, we have employed a hybrid QM/MM approach (B3LYP:UFF), wherein the molecule is divided into a 'core', treated at the quantum mechanical level, and a 'periphery', described using the more tractable molecular mechanics protocol. In our original 1998 work, we defined the core as $[Nb(Cl)(iPr)(HCCH)(NHCH_2)_3]^+$, implying cuts through the N−N, C−C, and C−Me bonds of the Tp^{Me2} ligand as well as the C−R bonds of the alkyne (Scheme 1, Model I). Such a dramatic simplification of the ligand is clearly far from ideal because replacing the anionic Tp^{Me2} ligand with three neutral imine groups introduces a positive charge in the QM partition. Moreover, making cuts across bonds with aromatic character necessarily leads to localization of the π character in the core partition and hence underestimation of N=C bond lengths. Such gross simpli-

fications were, however, necessary and pragmatic given the computational resources available when we started this work in 1998, and we were greatly encouraged by the apparently good agreement between experiment and theory, both in terms of structural parameters and the energetic separation of the different minima.[12]

Very recently, we turned our attention to the dynamic exchange between the different agostic rotamers, a problem that requires the accurate computation of transition structures as well as the minima we have considered previously. The rapid advances in hardware since our initial work mean that a full QM treatment of the whole system is now computationally tractable, and, given the deficiencies of the original QM/MM protocol highlighted in the previous paragraph, we decided that the time was right to adopt a full QM approach. As a starting point, we naturally reoptimized the equilibrium structures of the various minima using our apparently improved full QM protocol, expecting to see an even closer agreement with experimental structures and energies. To our great surprise, we discovered that the agreement was instead dramatically worse: in fact, a full QM calculation using the B3LYP functional and basis sets similar to those employed in our previous hybrid approach completely failed to locate an agostic minimum of any kind.

In view of this apparent failure of the B3LYP functional, we now report a systematic survey of density functionals, with the aim of establishing a suitable protocol for describing the agostic bonds in these systems. Although the performance of different density functionals is well documented in a variety of chemical contexts,[16] it seems that no systematic evaluation of their performance has been reported for agostic interactions. In this contribution, we show that only those functionals with correlation parts that obey the Uniform Electron Gas (UEG) limit lead to minima with an agostic structure. Moreover, these functionals reproduce certain structural features (bond lengths and angles) that were, in hindsight, rather poorly represented in our original B3LYP:UFF calculations. Ultimately, we conclude that functionals which do not obey the UEG limit fail completely to describe the balance between agostic and Nb−Cl π bonding in these systems.

Computational Methodology

Basis Sets. In view of the weak nature of agostic interactions it is important to address adequately the issue of basis set selection from the outset. Practical limitations arise due to the large size of the system, so we sought to ensure a high quality description of the most critical features while remaining within the limits of computational feasibility. We therefore chose the valence triple-ζ polarized basis sets of Ahlrichs (TZVP) for all the atoms of the alkyl moiety as well as Cl[17] and valence double-ζ polarized (SVP) basis sets for all atoms of the alkyne ligand and the Tp^{Me2} backbone, with unpolarized SV basis sets for Tp^{Me2} substituents.[18] Niobium was described with the [6s5p3d] SDD valence basis set and the quasi-relativistic ECP28MWB effective core potential of Andrae et al.[19]

QM/MM Calculations. Hybrid quantum mechanical/molecular mechanical calculations were carried out with the ONIOM method,[20] using the B3LYP functional[21−23] for the quantum mechanics partition and the UFF force field[24] for the molecular mechanics partition. Basis sets for the QM region were identical to those described above. Details regarding the different partitioning schemes used are described in detail in the text. All ONIOM calculations used microiterations[25] for the optimization procedure and did not employ electrostatic embedding.

DFT Methods. Twenty-four density functionals were included in our study, sampled from all current DFT implementations. LSDA was evaluated in the form of the SVWN5 functional.[26,27] GGA functionals tested include the nonempirical PBE functional of Perdew, Burke, and Ernzerhof;[28] the BP86 functional incorporating Becke (B88) exchange[29] and Perdew correlation;[30] two functionals based on Perdew−Wang 1991 correlation,[31] BPW91 and mPWPW91;[32] and three functionals with the Lee−Yang−Parr expression for correlation,[23] BLYP,[29] OLYP,[33] and G96LYP.[34] Also from the GGA family we assessed the highly parametrized HCTH/147 and HCTH/407 modifications[35,36] of the Hamprecht−Cohen−Tozer−Handy functional,[37] itself an elaboration of Beckes's 1997 10-parameter functional form.[38] Hybrid GGA functionals included in our study were B3LYP (20% HF exchange),[21−23] B3PW91,[21,22,31] O3LYP (11.61% HF exchange),[23,39] X3LYP (21.8% HF exchange),[23,40] mPW1PW91 (25% HF exchange),[31,32] mPW1LYP,[23,32] and PBE1PBE (25% HF exchange),[28] and also two functionals based on modifications of Becke's B97[38] expression, B97-2[41] (21% HF exchange) and B98[42] (21.98% HF exchange), were included. From the field of meta-GGA (τ-dependent) functionals we have tested the VSXC functional of van Voorhis and Scuseria[43] and the nonempirical functional of Tao, Perdew, Staroverov, and Scuseria (TPSS).[44] Last, from the hybrid-meta-GGA family we assessed Becke's B1B95 functional[45] (28% HF exchange), mPW1B95 (25% HF exchange), and TPSSh[46] (10% exact exchange).

We use the isopropyl complex, Tp^{Me2}NbCl(PhCCMe)*i*Pr, where structural data are available for the dominant β-C−H agostic isomer (Figure 1), as a test case for this study. The phenyl group of the alkyne was replaced by a methyl in the computational model in order to reduce computational cost; test calculations confirm that this simplification has negligible impact on the optimized structural parameters. Full geometry optimizations with no restrictions were carried out for each density functional. Calculations were initiated from either the experimental structure or from previously optimized geometries and were always allowed to proceed to convergence, even when initial divergence indicated the absence of a corresponding stationary point for a specific conformation. Optimized structures were confirmed to be genuine minima by analytic calculation of their harmonic vibrational frequencies. All calculations were performed with the Gaussian03 series of programs, Revision D.02.[47]

Results

In previous contributions we modeled the agostic complexes with QM/MM calculations of the IMOMM(B3LYP:UFF) type. As a first step in this systematic investigation, we have repeated these calculations using the same [Nb(Cl)(*i*Pr)-

Table 1. Optimized QM/MM (Models I−III) and Full QM (Model IV) Structural Parameters[c]

	$NbC_\alpha C_\beta$	$Nb-C_\beta$	$Nb-H_\beta$	$NbC_\alpha C_\beta H_\beta$	$C_\beta-H_\alpha$	$C_\beta-H'$ [b]	$Nb-C_\alpha$	$C_\alpha-C_\beta$	$C_\alpha-C'_\beta$	Nb−Cl
expt	87.0(3)	2.608(4)	2.17(5)	2.4	1.11(5)		2.228(4)	1.476(7)	1.535(6)	2.493(1)
					B3LYP:UFF					
Model I	90.7	2.734	2.366	1.0	1.110	1.091	2.250	1.528	1.524	2.428
Model II	107.7	3.126	2.976	14.2	1.092	1.093	2.282	1.552	1.531	2.423
Model III	110.1	3.177	3.087	25.0	1.090	1.094	2.291	1.549	1.532	2.430
Model IV	109.3	3.148	3.226	52.2	1.089	1.094	2.281	1.543	1.532	2.440
					PBE1PBE:UFF					
Model I	86.5	2.609	2.189	1.3	1.125	1.091	2.224	1.507	1.514	2.424
Model II	88.3	2.648	2.242	1.1	1.119	1.092	2.219	1.512	1.515	2.457
Model III	87.9	2.641	2.232	1.2	1.120	1.092	2.220	1.513	1.515	2.470
Model IV	87.2	2.620	2.204	3.5	1.123	1.091	2.217	1.511	1.514	2.494
					B3LYP:UFF on Zirconium Analogue					
Model I	110.1	3.266	3.218	40.0	1.091	1.097	2.399	1.540	1.532	2.529

[a] Bond length of agostic C−H bond or of C−H bond with the shortest Nb−H distance. [b] Mean value of the other two C−H bond lengths. [c] Angles in degrees, distances in Å.

$(HCCH)(NHCH_2)_3]^+$ 'core' but employing the larger basis sets described above and following the ONIOM(B3LYP:UFF) protocol (Scheme 1, Model I and Table 1). The QM region was then expanded in three steps to include the following: (i) the whole Tp backbone but not the methyl groups (Model II), (ii) the Tp backbone and the substituents on the alkyne (Model III), and (iii) the entire molecule (Model IV). The results for Model I are very similar to those reported in our original work, where the partition was identical but the basis set rather more limited. When we originally published these results, we were encouraged by the fact that the gross geometric features of the agostic unit were reproduced with reasonable accuracy with even this small core. A careful examination of bond lengths and angles, however, reveals a number of discrepancies, all of which can be traced to the partitioning of the system into a QM and an MM region. For example, the optimized N−C bond lengths of 1.28 Å are some 0.06 Å shorter than in the crystal structure—a direct consequence of the loss of aromatic character—while the C−C−C bond angles in the alkyne moiety are overestimated by approximately 10°. More subtly, the two C−C bond lengths are almost identical, whereas in the crystal structure the C−C bond in the agostic position ($C_\alpha-C_\beta$) is somewhat shorter than the other ($C_\alpha-C'_\beta$). Finally, but most importantly, the optimized Nb−Cl bond length is some 0.07 Å shorter than the experimental value, suggesting that Nb−Cl π bonding is overestimated in this case. Taken as a whole, these results imply a somewhat imbalanced description of the electronic structure within the Nb coordination sphere.

Incorporation of the Tp backbone and the alkyne substituents into the QM partition (Models II and III) eliminates the inaccuracies in the pyrazolyl N−C bond lengths (optimized values 1.34 Å) and alkyne angles. Surprisingly, however, these improvements come at the expense of the agostic interaction, which disappears completely: the agostic C−H bond length decreases from 1.110 Å (Model I) to 1.090 Å (Model III), while the $Nb-C_\beta$ distance increases from 2.734 Å to 3.177 Å. These changes are accompanied by rotation of the agostic methyl group which removes the hydrogen atom from the agostic plane. The full B3LYP calculation (Model IV) also fails to reproduce the agostic structure, converging instead to an anagostic minimum very similar to that of Model III, with an $Nb-C_\beta$ distance of 3.128 Å and an $NbC_\alpha C_\beta H_\beta$ dihedral of 52.2°. We emphasize that an agostic stationary point proved impossible to locate even after extensive sampling of the potential energy surface in the vicinity of the agostic structure. It should also be stressed that this result was unaffected by basis set extension (the Martin−Sundermann (2fg) polarization set[48] for Nb and a QZVP basis set for *i*Pr gave a similar structure), so we conclude that the source of this surprising failure is the density functional.

In order to obtain insight into the origin of this failure we undertook a systematic comparison of 24 distinct density functionals. Optimized structural parameters for all 24 are collected in Table 2. The functionals clearly fall into four distinct groups (A−D), based on the shape of the resultant potential energy surface (Figure 2). There are 11 density functionals that identify both an agostic and an anagostic minimum on the potential energy surface, six of which predict the agostic minimum to be more stable (group A: PBE1PBE, PBEPBE, B1B95, mPW1B95, TPSS, and TPSSh), while the other five (group B: BP86, BPW91, mPWPW91, B3PW91, and mPW1PW91) favor the anagostic structure, albeit only marginally. In the third group (C) we find two functionals (VSXC and SVWN5) that identify the agostic minimum but do not locate an anagostic alternative. The 11 functionals in the fourth group (D) predict the anagostic structure to be the unique minimum on the potential energy surface, failing completely to identify the experimentally observed agostic geometry. These functionals either incorporate the Lee−Yang−Parr (LYP) correlation or are based on modifications and extensions of the multiple-coefficient B97 functional (B98, B97-2, HCTH/147, and HCTH/407).

With the exception of SVWN5, the key optimized parameters for the agostic structure are very consistent among the first three groups of functionals: the agostic $C_\beta-H$ bonds are significantly elongated in all cases (1.12−1.13 Å), while the $Nb-C_\beta$ distances lie in the range 2.58−2.67 Å, in excellent agreement with the experimental value of 2.608(4) Å. The SVWN5 results are qualitatively correct, but the

Table 2. Structural Parameters of Agostic and Anagostic Minima[c]

		agostic						anagostic						
		$NbC_\alpha C_\beta$	$Nb-C_\beta$	$Nb-H_\beta$	$C_\beta-H^a$	$C_\beta-H'^b$	Nb−Cl	$NbC_\beta C_\beta$	$Nb-C_\beta$	$Nb-H_\beta$	$C_\beta-H^a$	$C_\beta-H'^b$	Nb−Cl	ΔE
	expt	87.0(3)	2.608(4)	2.17(5)	1.11(5)		2.493(1)							
A	PBE1PBE	87.2	2.620	2.204	1.123	1.091	2.494	107.5	3.082	3.138	1.090	1.095	2.419	0.4
	PBEPBE	86.8	2.640	2.213	1.131	1.098	2.502	106.5	3.089	3.112	1.098	1.102	2.428	0.8
	B1B95	85.6	2.581	2.145	1.124	1.087	2.494	104.7	3.017	3.050	1.088	1.092	2.416	7.5
	mPW1B95	85.7	2.581	2.149	1.123	1.086	2.490	104.6	3.009	3.048	1.087	1.090	2.415	8.3
	TPSS	86.3	2.634	2.189	1.129	1.093	2.502	107.0	3.106	3.129	1.093	1.097	2.429	2.7
	TPSSh	86.5	2.626	2.188	1.126	1.091	2.499	107.5	3.103	3.144	1.091	1.095	2.425	2.4
B	BP86	87.2	2.656	2.230	1.130	1.099	2.504	107.2	3.111	3.166	1.098	1.103	2.431	−0.4
	BPW91	87.3	2.658	2.234	1.128	1.097	2.503	107.4	3.115	3.160	1.096	1.101	2.428	−1.2
	B3PW91	87.9	2.647	2.238	1.120	1.090	2.496	108.0	3.102	3.152	1.090	1.095	2.422	−1.6
	mPWPW91	87.1	2.650	2.225	1.128	1.096	2.503	107.1	3.105	3.156	1.096	1.101	2.428	−0.3
	mPW1PW91	87.5	2.631	2.219	1.120	1.089	2.493	107.7	3.089	3.144	1.089	1.093	2.419	−0.6
C	VSXC	88.3	2.668	2.271	1.122	1.095	2.499							
	SVWN5	83.4	2.524	2.063	1.150	1.101	2.466							
D	B3LYP							109.3	3.148	3.226	1.089	1.094	2.440	
	O3LYP							109.7	3.157	3.215	1.088	1.094	2.419	
	X3LYP							109.2	3.143	3.226	1.089	1.094	2.440	
	mPW1LYP							109.5	3.149	3.235	1.088	1.093	2.443	
	BLYP							109.1	3.178	3.246	1.095	1.101	2.453	
	OLYP							110.0	3.179	3.234	1.091	1.097	2.419	
	G96LYP							109.1	3.172	3.223	1.094	1.100	2.445	
	B98							109.0	3.135	3.209	1.091	1.095	2.434	
	B97−2							108.7	3.120	3.184	1.088	1.093	2.421	
	HCTH/147							109.0	3.151	3.210	1.091	1.096	2.424	
	HCTH/407							109.5	3.162	3.225	1.089	1.095	2.419	

[a] Bond length of agostic C−H bond or of C−H bond with the shortest Nb−H distance. [b] Mean value of the other two C−H bond lengths. [c] Angles in degrees, distances in Å, relative energies in kJ mol^{-1}.

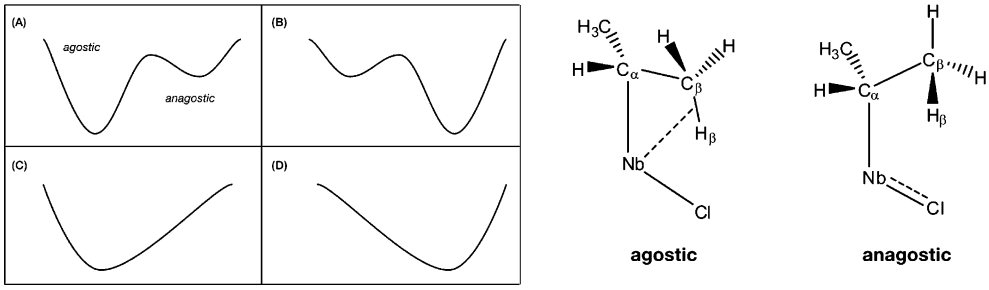

Figure 2. Schematic depiction of the topology of the potential energy for the four different groups of density functionals (A−D).

optimized parameters suggest that pure LSDA overestimates the strength of the agostic interaction. VSXC also identifies the agostic structure as the sole stationary point on the PES, but in this case the structure agrees more closely with both the experimental data and the predictions of the other functionals in groups A and B. The optimized structural parameters for the anagostic structure are also quite similar across groups A, B, and D: the $NbC_\alpha C_\beta$ angle is always wider than 104.5°, and in the case of group D functionals it is consistently between 109° and 110°. Comparison of the agostic and anagostic geometries for groups A and B reveals that the $Nb-C_\beta$ distance is about 0.5 Å longer in the anagostic isomer. The terminal methyl group in the anagostic structure is also rotated along the $C_\alpha-C_\beta$ axis so as to place the closest H_β atom a further 0.9 Å away from the metal center. Most significantly, the Nb−Cl bond length is always about 0.07 Å shorter in the anagostic structure, suggesting that π-donation from the chloride ligand competes with the agostic bond for vacant orbital space on the Nb center. A Natural Bond Orbital (NBO)[49] analysis of the agostic and anagostic structures (PBE1PBE) clearly illustrates this competition. The dominant donor−acceptor interaction between the $C_\beta-H$ σ bonding orbital and a formally empty Nb d orbital (99.6 kJ mol^{-1}) in the agostic structure disappears almost completely at the anagostic minimum (7.1 kJ mol^{-1}) and is replaced by an interaction of similar magnitude between a chloride lone pair and the same Nb d orbital (58.6 kJ mol^{-1}).

The direct competition between agostic interactions and Nb−Cl π bonding means that the Nb−Cl bond length provides a sensitive probe of the strength of the agostic bond: a short Nb−Cl bond in the region of 2.42 Å indicates weak (or nonexistent) agostic bonding, while a bond length around 2.49 Å is more consistent with a significant attraction between the metal and the C−H bond. This conclusion further increases our uneasiness about the small QM/MM

partition (Model I) used in our previous work, where we noted that the optimized Nb−Cl bond length was precisely 0.07 Å shorter than experiment. The optimized structure of the isopropyl complex (Table 1) therefore appears to feature *both* a strong agostic interaction (C−H 1.110 Å, Nb−H_β = 2.366 Å) *and* a strong Nb−Cl π bond (2.428 Å), despite the fact that the two electron pairs (C−H σ and Cl lone pair) are competing for a single vacant orbital on the metal.[11] We will return to this issue in our concluding remarks.

Close inspection of the members in each group of functionals reveals certain regularities that lead us to an understanding of the decisive factor governing the performance of the DFT methods. First of all, we see that all functionals that incorporate the Lee, Yang, and Parr (LYP) correlation[23] belong to group D and therefore fail to locate the agostic minimum. It is clear from Table 2 that the performance of LYP-containing methods remains the same irrespective of the exchange functional (pure GGA or hybrid) and regardless of the percent of exact exchange in the latter. The minimal effect of the exchange functional is also apparent in the other groups: for example, there is little difference between BPW91 and B3PW91 or between TPSS and TPSSh. The poor performance of the group D functionals can be traced to the approximations used to generate the correlation functionals. In the local density approximation (LDA) the exchange and correlation energies of a system at a given point in space are assumed to be those of a homogeneous electron gas of uniform density at that point. Consequently, LDA provides the correct results for uniform densities, or, in other words, it satisfies the uniform electron gas (UEG) limit. It also performs well for slowly varying densities, but in cases of more rapid density variations which are typical of molecular systems it usually underestimates the exchange energy and significantly overestimates the correlation energy. This deficiency is addressed by the generalized gradient approximation (GGA) functionals, which are usually constructed as corrections of the LDA with terms that depend on the gradients of the density. What distinguishes LYP from other correlation functionals of this kind is that it was not formulated as a correction of LDA but was instead constructed by recasting the Colle−Salvetti correlation energy formula of the helium atom[50] in terms of gradient expansions. Thus, LYP does not obey the uniform electron gas (UEG) limit. The other four members of group D share the same feature: B98 and B97-2 as well as the HCTH functionals are all based on the B97 functional, which does not satisfy the UEG limit. Conversely, the correlation parts of density functionals that successfully identify an agostic minimum (groups A, B, and C) do obey the UEG condition. These include the Perdew family of P86, PW91, and PBE GGA functionals as well as the meta-GGA correlation functionals B95 and TPSS. The only apparent exception to the rule regarding the UEG limit requirement is the VSXC functional, which, along with SVWN5, is the only one to locate only the agostic minimum. VSXC was developed on the basis of the density matrix expansion to model the exchange-correlation hole and in order to improve performance for molecular systems the UEG constraint was relaxed by reducing the LDA coefficients to 70% for opposite-spin and 33% for same-spin correlation. Despite that, VSXC manages to reproduce the agostic structure quite accurately, yielding only a marginally wider agostic angle compared to the other functionals. Therefore, the failure of group D functionals to predict a stationary point corresponding to the agostic structure can be traced to their divergence from the uniform electron gas (UEG) limit. We note that Schaeffer and co-workers have recently reported similar trends in a study of Ag_3 and Ag_4 clusters, where non-UEG functionals also yield poor results.[51] The nature of the bonding in these silver clusters is clearly rather different from the agostic interactions that are the focus of this study, suggesting that the choice of correlation functional may have important implications in a wider variety of chemical contexts.

A complementary perspective on the role of correlation can be obtained from wave function-based ab initio approaches. HF optimizations locate only the anagostic structure ($\angle NbC_\alpha C_\beta$ = 112.7°, Nb−C_β = 3.205 Å). Geometry optimizations at the MP2 level were not computationally feasible, so we chose to perform the comparison using single-point energy calculations on typical agostic and anagostic structures (optimized using the PBE1PBE functional). At the HF level the anagostic structure is 30.1 kJ mol^{-1} lower in energy than the agostic one, but the order is reversed at the MP2 level: the agostic structure is estimated to be 11.0 kJ mol^{-1} more stable than the anagostic one, an energy difference comparable to that predicted by the B95-based hybrid meta-GGA functionals. This stabilization of the agostic structure by 40 kJ mol^{-1} at the MP2 level emphasizes the importance of a correct description of dynamic correlation.

Having established that non-UEG correlation functionals are poorly suited to describing the agostic interactions in this class of systems, we can now return to our original hybrid QM/MM results and ask why we obtained apparently good results using this functional in combination with the highly simplified Model I partition. We have noted previously that a close inspection of the optimized structure of Model I (Table 1) reveals inconsistencies, the most serious being the short Nb−Cl bond, which effectively blocks donation of electron density from the C−H bond to the metal. So why then do we also observe a short Nb−H_β separation, generally considered to be characteristic of an agostic interaction? The answer lies in the simplifications implicit in our Model I QM/MM partition and, in particular, the presence of a positive charge in the QM region. This introduces an unphysical electrostatic component to the agostic interaction, which is sufficient to hold the C−H bond in the vicinity of the metal center even in the absence of significant charge transfer between the C−H bond and the Nb center. The electrostatic nature of the agostic interaction in this case is reflected in the agostic C−H bond length of 1.110 Å which, although longer than its nonagostic counterpart (1.091 Å), is still significantly shorter than those predicted by the group A functionals (1.12−1.13 Å). The impact of the spurious positive charge in the QM region is clearly illustrated by a further series of calculations on Models I−IV using the PBE1PBE functional (Table 1) where, in contrast to B3LYP,

the functional *does* provide a good description of the agostic bond at the full QM limit (Model IV). The competition between agostic and Nb−Cl π bonding for vacant orbital space is apparent in the trends in $C_\beta-H_\beta$, Nb−H_β, and Nb−Cl bond lengths in Models IV−II, all of which have a neutral QM region: the contraction of the Nb−Cl bond (2.494−2.457 Å) is accompanied by an increase in Nb−H_β (2.204−2.242 Å) and a decrease in $C_\beta-H_\beta$ (1.123−1.119 Å). The Nb−Cl bond length for Model I is even shorter, at 2.424 Å, and is typical of an anagostic structure. On the basis of the competition for vacant orbital space on Nb that we have emphasized above, we would therefore anticipate a further contraction of $C_\beta-H_\beta$ in Model I, along with an increase in Nb−H_β. In fact, precisely the opposite is observed: the $C_\beta-H_\beta$ bond length increases to 1.125 Å while the Nb−H_β bond length contracts to 2.189 Å. This discontinuity in structural trends provides clear evidence that the electronic mechanism responsible for holding the C−H bond close to the metal center is fundamentally different in Model I and Models II−IV. As a final confirmation of the critical role of the positive charge, we have optimized the structure of the isoelectronic zirconium complex, [Tp^{Me2}ZrCl(MeCCMe)*i*Pr]$^-$, using the Model I partition, where the QM region is now neutral rather than cationic. At the (B3LYP:UFF) level, this gives an anagostic minimum, quite distinct from the Model I niobium analogue (Table 1). We therefore conclude that the apparent success of our early B3LYP:UFF hybrid calculations was a result of the presence of a positive charge into the QM partition, which introduces an unrealistic electrostatic component to the agostic interaction. This additional attractive component compensates for the intrinsically imbalanced description of agostic and Nb−Cl π bonding afforded by this and other non-UEG functionals and leads to structures in qualitative agreement with experiment. Only a very close inspection of the niobium coordination sphere reveals the telltale signs of error compensation.

Conclusions

The calculations reported in this paper suggest that functionals that obey the UEG correlation limit provide an accurate picture of the subtle balance between Nb···C−H agostic and Nb−Cl π bonding in [Tp^{Me2}NbCl(MeCCMe)-*i*Pr] and so give excellent structure predictions. In contrast, functionals that do not obey the UEG limit appear to overestimate the strength of the Nb−Cl π bond relative to the agostic Nb···C−H, leading to anagostic structures, at odds with experiment. The popular B3LYP functional falls into the second category, and so these results serve a warning that this functional may be inappropriate, at least in cases where a competition between agostic and π-donor interactions for vacant orbital space is important. Somewhat surprisingly, an agostic structure is recovered by the B3LYP functional when the system is greatly simplified using the QM/MM methodology but only in cases where a positive charge is present in the QM region. The positive charge introduces an additional but unphysical electrostatic component to the agostic interaction which holds the C−H bond close to the metal even though strong Nb−Cl π bonding effectively blocks any sharing of electron density. The net result is an apparently good agreement with experiment, but only if we restrict our attention to the gross features of the alkyl chain. Our experience serves as a clear warning that the optimization of an 'agostic structure' in apparently good agreement with experiment does not necessarily mean that the chosen theoretical method has captured the true nature of the 'agostic bond'. It may instead simply reflect the fact that distortion of the angles within the alkyl group is relatively easy, and so a wide range of physical mechanisms can induce the bending regarded as typical of an agostic structure. The true nature of the agostic interaction is, however, revealed by the more subtle features of the metal coordination sphere, in this case the Nb−Cl bond length, which acts as a sensitive indicator of the presence or absence of shared electron density between the C−H bond and the metal center.

References

(1) Brookhart, M.; Green, M. L. H. *J. Organomet. Chem.* **1983**, *250*, 395.

(2) Brookhart, M.; Green, M. L. H.; Wong, L. L. *Prog. Inorg. Chem.* **1988**, *36*, 1.

(3) Clot, E.; Eisenstein, O. *Struct. Bonding* **2004**, *113*, 1.

(4) (a) Cotton, F. A.; Stanislowski, A. G. *J. Am. Chem. Soc.* **1974**, *96*, 754. (b) Cotton, F. A. *Inorg. Chem.* **2002**, *41*, 643.

(5) (a) Eisenstein, O.; Jean, Y. *J. Am. Chem. Soc.* **1985**, *107*, 1177. (b) Demolliens, A.; Jean, Y.; Eisenstein, O. *Organometallics* **1986**, *5*, 1457.

(6) Popelier, P. L. A.; Logothetis, G. *J. Organomet. Chem.* **1998**, *555*, 101.

(7) Scherer, W.; McGrady, G. S. *Angew. Chem., Int. Ed.* **2004**, *43*, 1782.

(8) (a) Haaland, A.; Scherer, W.; Ruud, K.; McGrady, G. S.; Downs, A. J.; Swang, O. *J. Am. Chem. Soc.* **1998**, *120*, 3762. (b) Scherer, W.; Priermeier, T.; Haaland, A.; Volden, H. V.; McGrady, G. S.; Downs, A. J.; Boese, R.; Bläser, D. *Organometallics* **1998**, *17*, 4406. (c) Scherer, W.; Hieringer, W.; Spiegler, M.; Sirsch, P.; McGrady, G. S.; Downs, A. J.; Haaland, A.; Pedersen, B. *Chem. Commun.* **1998**, 2471.

(9) (a) Butts, M. D.; Bryan, J. C.; Luo, X.-L.; Kubas, G. *Inorg. Chem.* **1997**, *36*, 3341. (b) Nikonov, G. I.; Mountford, P.; Ignatov, S. K.; Green, J. C.; Leech, M. A.; Kuzmina, G. L.; Razuvaev, A. G.; Rees, N. H.; Blake, A. J.; Howard, J. A. K.; Lemenovskii, D. A. *J. Chem. Soc., Dalton Trans.* **2001**, 2903.

(10) (a) Ziegler, T.; Tschinke, V.; Becke, A. *J. Am. Chem. Soc.* **1987**, *109*, 1351. (b) Han, Y.; Deng, L.; Ziegler, T. *J. Am. Chem. Soc.* **1997**, *119*, 5939.

(11) Jaffart, J.; Mathieu, R.; Etienne, M.; McGrady, J. E.; Eisenstein, O.; Maseras, F. *J. Chem. Soc., Chem. Commun.* **1998**, 2011.

(12) Jaffart, J.; Etienne, M.; Maseras, F.; McGrady, J. E.; Eisenstein, O. *J. Am. Chem. Soc.* **2001**, *123*, 6000.

(13) Jaffart, J.; Etienne, M.; Reinhold, M.; McGrady, J. E.; Maseras, F. *Chem. Commun.* **2003**, 876.

(14) Jaffart, J.; Cole, M. L.; Etienne, M.; Reinhold, M.; McGrady, J. E.; Maseras, F. *Dalton Trans.* **2003**, 4057.

(15) Besora, M.; Maseras, F.; McGrady, J. E.; Oulié, P.; Dinh, D. H.; Duhayon, C.; Etienne, M. *Dalton Trans.* **2006**, 2362.

(16) (a) Riley, K. E.; Op't Holt, B. T.; Merz, K. M., Jr. *J. Chem. Theory Comput*. **2007**, *3*, 407. (b) Jacquemin, D.; Femenias, A.; Chermette, H.; Ciofini, I.; Adamo, C.; André, J.-M.; Perpète, E. A. *J. Phys. Chem. A* **2006**, *110*, 5952. (c) Zhao, Y.; Truhlar, D. G. *J. Chem. Phys.* **2006**, *124*, 224105. (d) Zhao, Y.; Truhlar, D. G. *J. Chem. Theory Comput*. **2005**, *1*, 415. (e) Brothers, E. N.; Merz, K. M., Jr. *J. Phys. Chem. A* **2004**, *108*, 2904. (f) Raymond, K. S.; Wheeler, R. A. *J. Comput. Chem*. **1999**, *20*, 207. (g) Ghosh, A.; Taylor, P. R. *Curr. Opin. Chem. Biol*. **2003**, *7*, 113. (h) Holthausen, M. C. *J. Comput. Chem.* **2005**, *26*, 1505. (i) Buhl, M.; Kabrede, H. *J. Chem. Theory Comput.* **2006**, *2*, 1282. (j) Schultz, N. E.; Zhao, Y.; Truhlar, D. G. *J. Phys. Chem. A* **2005**, *109*, 11127.

(17) Schäfer, A.; Huber, C.; Ahlrichs, R. *J. Chem. Phys.* **1994**, *100*, 5829.

(18) Schäfer, A.; Horn, H.; Ahlrichs, R. *J. Chem. Phys.* **1992**, *97*, 2571.

(19) Andrae, D.; Haeussermann, U.; Dolg, M.; Stoll, H.; Preuss, H. *Theor. Chim. Acta* **1990**, *77*, 123.

(20) (a) Maseras, F.; Morokuma, K. *J. Comput. Chem.* **1995**, *16*, 1170. (b) Dapprich, S.; Komaromi, I.; Byun, K. S.; Morokuma, K.; Frisch, M. J. *J. Mol. Struct. (Theochem)* **1999**, *461*, 1.

(21) Becke, A. D. *J. Chem. Phys.* **1993**, *98*, 5648.

(22) Stevens, P. J.; Devlin, J. F.; Chabalowski, C. F.; Frisch, M. J. *J. Phys. Chem.* **1994**, *98*, 11623.

(23) Lee, C.; Yang, W.; Parr, R. G. *Phys. Rev. B* **1988**, *37*, 785.

(24) Rappé, A. K.; Casewit, C. J.; Colwell, K. S.; Goddard, W. A., III; Skiff, W. M. *J. Am. Chem. Soc.* **1992**, *114*, 10024.

(25) Vreven, T.; Morokuma, K.; Farkas, Ö.; Schlegel, H. B.; Frisch, M. J. *J. Comput. Chem.* **2003**, *24*, 760.

(26) Slater, J. C. *Quantum Theory of Molecules and Solids, Vol. 4: The Self-Consistent Field for Molecules and Solids*; McGraw-Hill: New York, 1974; pp 12−79.

(27) Vosko, S. J.; Wilk, L.; Nusair, M. *Can. J. Chem.* **1980**, *58*, 1200.

(28) Perdew, J. P.; Burke, K.; Ernzerhof, M. *Phys. Rev. Lett.* **1996**, *77*, 3865.

(29) Becke, A. D. *Phys. Rev. A* **1988**, *38*, 3098.

(30) Perdew, J. P. *Phys. Rev. B* **1986**, *33*, 8822.

(31) Perdew, J. P.; Wang, Y. *Phys. Rev. B* **1992**, *45*, 13244.

(32) Adamo, C.; Barone, V. *J. Chem. Phys.* **1998**, *108*, 664.

(33) Handy, N. C.; Cohen, A. J. *Mol. Phys.* **2001**, *99*, 403.

(34) Gill, P. M. W. *Mol. Phys.* **1996**, *89*, 433.

(35) Boese, A. D.; Doltsinis, N. L.; Handy, N. C.; Sprik, M. *J. Chem. Phys.* **2000**, *112*, 1670.

(36) Boese, A. D.; Handy, N. C. *J. Chem. Phys.* **2001**, *114*, 5497.

(37) Hamprecht, F. A.; Cohen, A. J.; Tozer, D. J.; Handy, N. C. *J. Chem. Phys.* **1998**, *109*, 6264.

(38) Becke, A. D. *J. Chem. Phys.* **1997**, *107*, 8554.

(39) Cohen, A. J.; Handy, N. C. *Mol. Phys.* **2001**, *99*, 607.

(40) Xu, X.; Goddard, W. A. *Proc. Natl. Acad. Sci. U.S.A.* **2004**, *101*, 2673.

(41) Wilson, P. J.; Bradley, T. J.; Tozer, D. J. *J. Chem. Phys.* **2001**, *115*, 9233.

(42) Schmider, H. L.; Becke, A. D. *J. Chem. Phys.* **1998**, *108*, 9624.

(43) van Voorhis, T.; Scuseria, G. E. *J. Chem. Phys.* **1998**, *109*, 400.

(44) Tao, J.; Perdew, J. P.; Staroverov, V. N.; Scuseria, G. E. *Phys. Rev. Lett.* **2003**, *91*, 146401.

(45) Becke, A. D. *J. Chem. Phys.* **1996**, *104*, 1040.

(46) Staroverov, V. N.; Scuseria, G. E.; Tao, J.; Perdew, J. P. *J. Chem. Phys.* **2003**, *119*, 12129.

(47) Frisch, M. J.; Trucks, G. W.; Schlegel, H. B.; Scuseria, G. E.; Robb, M. A.; Cheeseman, J. R.; Montgomery, J. A., Jr.; Vreven, T.; Kudin, K. N.; Burant, J. C.; Millam, J. M.; Iyengar, S. S.; Tomasi, J.; Barone, V.; Mennucci, B.; Cossi, M.; Scalmani, G.; Rega, N.; Petersson, G. A.; Nakatsuji, H.; Hada, M.; Ehara, M.; Toyota, K.; Fukuda, R.; Hasegawa, J.; Ishida, M.; Nakajima, T.; Honda, Y.; Kitao, O.; Nakai, H.; Klene, M.; Li, X.; Knox, J. E.; Hratchian, H. P.; Cross, J. B.; Bakken, V.; Adamo, C.; Jaramillo, J.; Gomperts, R.; Stratmann, R. E.; Yazyev, O.; Austin, A. J.; Cammi, R.; Pomelli, C.; Ochterski, J. W.; Ayala, P. Y.; Morokuma, K.; Voth, G. A.; Salvador, P.; Dannenberg, J. J.; Zakrzewski, V. G.; Dapprich, S.; Daniels, A. D.; Strain, M. C.; Farkas, O.; Malick, D. K.; Rabuck, A. D.; Raghavachari, K.; Foresman, J. B.; Ortiz, J. V.; Cui, Q.; Baboul, A. G.; Clifford, S.; Cioslowski, J.; Stefanov, B. B.; Liu, G.; Liashenko, A.; Piskorz, P.; Komaromi, I.; Martin, R. L.; Fox, D. J.; Keith, T.; Al-Laham, M. A.; Peng, C. Y.; Nanayakkara, A.; Challacombe, M.; Gill, P. M. W.; Johnson, B.; Chen, W.; Wong, M. W.; Gonzalez, C.; Pople, J. A. *Gaussian 03, Revision D.02*; Gaussian, Inc.: Wallingford, CT, 2004.

(48) Martin, J. M. L.; Sundermann, A. *J. Chem. Phys.* **2001**, *114*, 3408.

(49) (a) Weinhold, F.; Landis, C. *Valency and Bonding. A Natural Bond Orbital Donor-Acceptor Perspective*; Cambridge University Press: Cambridge, U.K., 2005; pp 45−86. (b) Glendening, E. D.; Badenhoop, J. K.; Reed, A. E.; Carpenter, J. E.; Bohmann, J. A.; Morales, C. M.; Weinhold, F. *NBO 5. G*; Theoretical Chemistry Institute, University of Wisconsin: Madison, WI, 2001.

(50) Colle, R.; Salvetti, D. *Theor. Chim. Acta* **1975**, *37*, 329.

(51) Zhao, S.; Li, Z.-H.; Wang, W.-N.; Liu, Z.-P.; Fan, K.-N.; Xie, Y.; Schaefer, H. F., III *J. Chem. Phys.* **2006**, *124*, 184102.

CT700043W